J. comp. Physiol. 119, 73–84 (1977)

Journal of Comparative Physiology · A

The Superposition Image in the Eye of *Ephestia kühniella*

P. Cleary, G. Deichsel, and P. Kunze

Biologisches Institut der Universität Stuttgart, Abteilung Tierphysiologie, Ulmer Straße 227, D-7000 Stuttgart 60, Federal Republic of Germany

Received February 24, 1977

Summary. Superposition images according to Exner (1891) are observed behind fresh eye-cups of *Ephestia* which were mounted with gelatine on a cover-glass and kept in a moist chamber. Their position was determined as 125 ± 15 µm proximal to the crystalline cone tip having made allowance for the passage of light through media of different refractive indices. This distance places the image in the rhabdom layer as determined by histology. The same holds for the superposition image constructed from calculated ray paths in the dioptric system of *Ephestia*. The computer aided calculation was based on refractive index measurements in cornea and cone. It was carried out by applying Snell's law for infinitesimally thin sections. The dioptric system shows properties analogous to a Kepler telescope adjusted for infinity. Parallel incoming light with an angle of up to 22° to the axis is focused in a plane about half way down the cone and leaves the cone again in direction of the rhabdom layer almost parallel. The angular magnification of the system is 1.32.

Introduction

The superposition principle of image formation in arthropod eyes requires an erect ray path in the optical systems of the ommatidia (Exner, 1891). This erect ray path can be produced by an inhomogeneous refractive index distribution which is radially symmetrical to the axis of the optical system.

The eye of *Ephestia kühniella* was shown by various optical and behavioural tests to be of the superposition type (Kunze, 1972a). Refractive index measurements in the cone (Kunze and Hausen, 1971; Hausen, 1973) and in the cornea (Vogt, 1974) revealed a highly inhomogeneous system with imaging properties.

In such an eye the optical systems of different ommatidia combine in forming the superposition image of a distant object by the intersection of ray bundles (Exner, 1891). For optimal perception of this image the ray bundles should be expected to intersect close to or in the rhabdom layer.

Although in *Ephestia* the existence of a superposition image was reported (Kunze, 1969) its position in the eye is not known. In this paper, the position of the superposition image is determined in two ways: a) The superposition image is directly observed in eye-cup preparations and its distance from the dioptric apparatus determined. b) The ray path in the dioptric system is computed on the basis of the refractive index measurements in cornea (Vogt, 1974) and cone (Hausen, 1973) applying Snell's law for infinitesimally thin layers; the resulting rays are used for the construction of the superposition image. Both image determinations are related to the anatomy of the *Ephestia* eye (Fischer and Horstmann, 1971).

Methods

a) Eye-Cup Preparations

The head and most of the thorax of a fresh specimen of *Ephestia kühniella* (mutant *transparent*, without screening pigment) were firmly affixed to the end of a small brass tube with wax/rosin and thus completely immobilised; one eye was left free. The tube was mounted in a micromanipulator, and under a stereomicroscope a cup approximately 30 facets in diameter was cut from this eye with a vibrating razor blade. The eye-cup floated on a drop of Ringer solution from which it was transferred to a drop of fresh gelatine solution (ca. 2.5%) on a cover slide. The gelatine solution had been kept at 40 °C. Having been transferred to the cover glass it cooled down and stabilized the attached eye cup. We assumed the refractive index of the gelatine solution ($n=1.339$ at room temperature) to be close to that of the clear zone in the intact eye. The slide was inverted to form the lid of a shallow moist-chamber; the lower face of the chamber was also a cover-slide. The device was placed under an incident light microscope which was equipped with a high sensitivity electronic gauge for depth measurement. Four miniature light bulbs (arranged like a number 1, the most distant bulbs being 1.5 cm apart) in front of the preparation served as a test object for light propagation by the dioptric systems of the eye-cup. Each preparation was checked for undisturbed hexagonal arrangement of the dioptric systems. Minor dislocations of single cones were neglected. Preparations containing air bubbles were discarded.

b) Ray Tracing

The refractive index distribution was assumed to be radially symmetric. Our calculations are based on plane axial sections through the cornea and crystalline cone. A cartesian x–y system of axes was introduced (Fig. 4) with the x-axis being the symmetry axis and the point (0,0) the distal cornea apex.

Geometry. The cornea and crystalline cone are radially symmetrical. The generating curves are, for the cornea, a circular arc ($r=14$ µm) and straight lines parallel and perpendicular to the axis. Radius measurements of the crystalline cone were only taken at 16 discrete points (Hausen, 1973, Fig. 4b). A polynominal of 9th degree proved to be suitable as generating curve; its coefficients were calculated from the 16 data points using the least squares method. The distal end of the cone was approximated by an elliptical arc with the apex on the axis.

Refractive Index Distribution. The equations used were for the cornea

$$n(x,y)=a_0+a_1x+a_2x^2+a_3y^2+a_4x^3+a_5xy^2,$$

and for the crystalline cone

$$n(x,y)=b_0+b_1x+b_2x^2+b_3y^2+b_4x^3+b_5xy^2+b_6x^4+b_7x^2y^2.$$

The coefficients were estimated by the method of least squares from data in Vogt (1974, Fig. 3a) for the a_i, and Hausen (1973, Fig. 4) for the b_i. The difference between a model and a measured refractive index was always less than 0.01.

Calculation of the Ray Path. The ray path was approximated as a series of arcs. The radius of each arc was calculated by the iterative application of Snell's law for infinitesimally thin layers. The formula used

$$\frac{1}{\rho} = -\frac{1}{n} \cdot \frac{dn}{dr}$$

was taken from Gerthsen (1966, p. 301) (with ρ being the radius of the approximating arc, n the refractive index, and dr the part of ρ which extends through dn). Essentially the same method was used by Megitt and Meyer-Rochow (1975) for ray processing in arthropod eyes. The TR 440 computer at the Institut für Informatik, University of Stuttgart, enabled us to calculate and plot eight rays in one run. Input data for each set of rays were: 1) the starting coordinates, 2) the starting angles with the axis, 3) the length of the approximating arcs, 4) the cornea cone distance, 5) the refractive index of the eye medium.

Experiments and Results

a) Measurements on Eye-Cup Preparations

We determined in each preparation the positions of the cover-glass surfaces, central cone tip, and superposition image. The position of the image we judged by the best contrast. In many cases the cone tip was not readily discernable. However, in good preparations both cone tip and exit pupil of the entire dioptric system could be observed and were measured to be within 5 µm of one another. Therefore the cone tip was regarded as coincident with the exit pupil, and the pupil measured as such.

In our preparations the observed light rays, after leaving the crystalline cones, traverse the phase boundaries eye-cup-contents/cover-glass, and cover-glass/objective-medium. By refraction their angle with the microscope axis is changed according to Snell's law. This change must be taken into account in determining the real depths of observed objects or images.

In Figure 1 possible ray paths in an eye-cup preparation are shown: The ray bundles from cone tips C and D intersect in situ at point S, there forming the superposition image. When the eye-cup is placed on a cover-glass ($n_2 > n_3$) the rays are refracted so that they intersect at S′. This point is optically shifted to S″ by the phase transition n_2 to n_1. Similary C is observed at C'. The wanted distance CS is changed by refraction to the observed distance $C'S''$. It can easily be shown that for rays at small angles to the microscope axis the distance $CS = C'S'' n_3/n_1$.

Thus, measurements in eye-cup preparations on cover-glasses with oil immersion or dry objectives can yield considerable errors (more than 50% in depth determinations) if not corrected. Most of our measurements were performed with a water immersion objective (n.a. = 0,75). We regarded the refractive index of our gelatine solution and of the eye-cup-contents to be close enough to that of water to dispense with a correction. Several measurements made for comparison with a dry objective, and corrected in the above way, confirmed this.

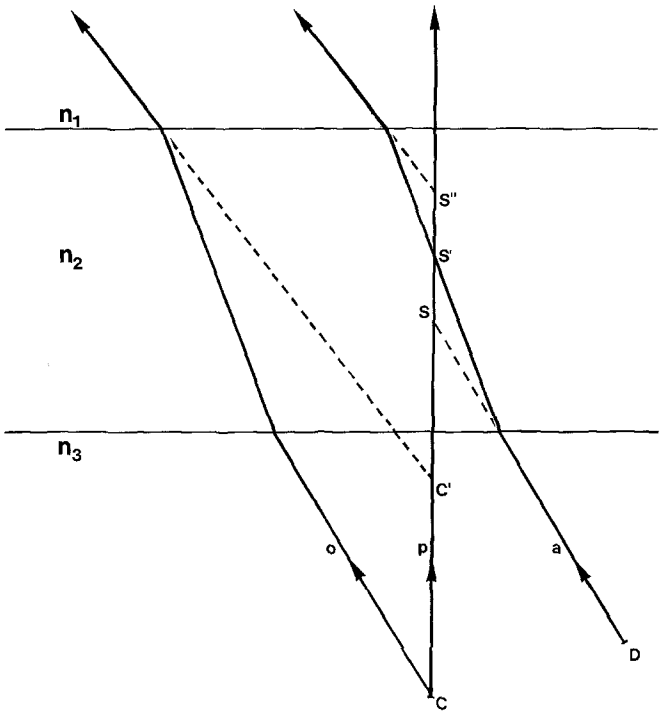

Fig. 1. Refraction of rays o, p, a from cone tips C and D when passing through media of different refractive indices ($n_2 > n_3 > n_1$). Rays p and a are exit rays for parallel incident light; they form the superposition image S

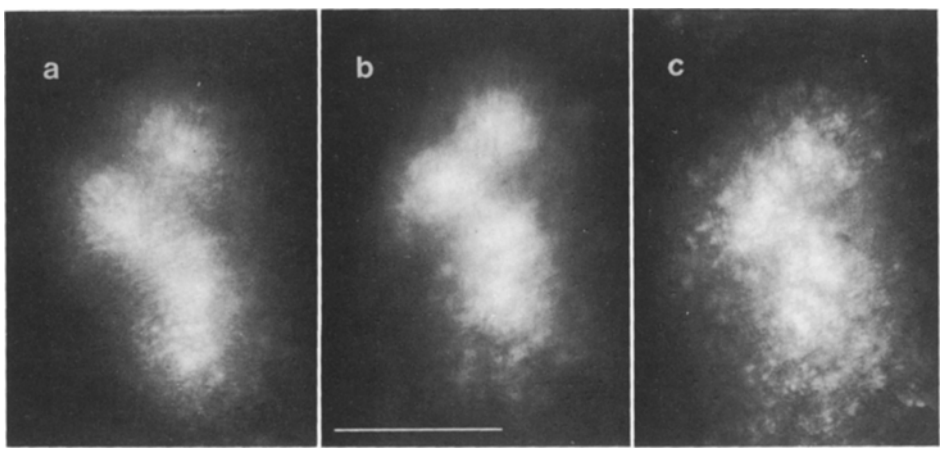

Fig. 2a–c. Superposition images behind one eye-cup preparation. They were photographed at **a** 110 μm (image in gelatine), **b** 130 μm (image in glass), and **c** 150 μm (image in glass) proximal to the central crystalline cone tip. Photographs were taken with Kodak 2475 Recording Film and produced on soft paper with equal exposure times for **a–c**. Marker 50 μm

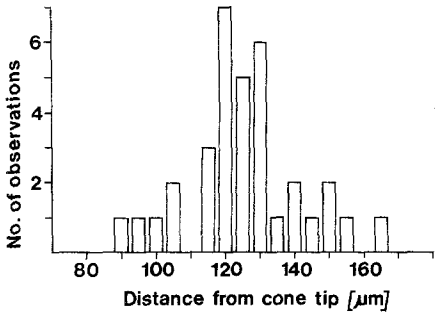

Fig. 3. Depth distribution of superposition images (as in Fig. 2b) observed in 21 different preparations

Figure 2 presents photographs of observed images. The object was 33 mm in front of the eye. The photographs were taken in the same preparation at 20 μm depth intervals. They vary in extension, contrast, and distinctness. The same variation was observed in all our preparations. The image in Figure 2b appears to be the least extended and most contrasty. The image with these properties was chosen as the superposition image. It was found either in the cover-glass (as the one in Fig. 2b) or in gelatine. Its distance from the crystalline cone tip was determined.

The depth distribution of the superposition images is presented in Figure 3. The distances from the cone tip at which we found superposition images ranged from 90 μm to 165 μm with a mean of 125 ± 15 μm (standard deviation). From a total of 34 measured images 21 were found between 115 and 135 μm.

b) Ray Tracing

The length of the approximating arcs was varied in test runs with the result that arc lengths shorter than 1 μm did not change the computed ray paths. Thus, an arc length of 1 μm was used in all following calculations.

Satisfactory experimental data on the eye medium in contact with the proximal cornea and around the crystalline cone are not available at present. Also the cornea cone distance is only known to be in the range 3–5 μm (Fischer and Horstmann, 1971, and own histological observations). Test runs for (homogeneous) eye medium indices from 1.34 to 1.38 in combination with cornea cone distances of 3 and 5 μm revealed no striking differences for the different combinations. Consequently we present data only for an eye medium with $n = 1.36$ (approx. the mean between water and the cone edge refractive index), and for a cornea cone distance of 5 μm.

The starting positions of the input rays ($x = 0$) ranged from $y = -8$ μm to $y = +8$ μm in steps of 2 μm with the exception of $y = +2$ μm which was omitted due to the limitation to eight rays for one run. Input angles (α) were varied from 0° in steps of 3°.

Rays which after passing the cornea did not enter the crystalline cone or which suffered total reflection at the cone boundary were not processed further. (Such rays will be discussed later.)

Table 1. Position and angle of exit rays for input rays from 0 to 21°

α	0°		3°		6°		9°	
y_i	y_e	β	y_e	β	y_e	β	y_e	β
8	–	–	–	–	–	–	–	–
6	−3.9	−1.1	−3.8	2.4	−3.5	6.0	−3.3	9.9
4	−2.6	0.4	−2.4	4.0	−2.2	7.5	−2.0	12.1
2	−1.3	0.7	−1.1	4.2	−0.9	8.2	−0.7	11.7
0	0	0	0.2	3.2	0.4	6.8	0.6	10.5
−4	2.6	−0.4	2.8	3.1	3.0	6.7	3.2	11.0
−6	3.9	1.1	4.1	4.5	4.3	7.9	4.5	12.3
−8	–	–	–	–	5.8	10.5	6.0	14.2
	12°		15°		18°		21°	
8	–	–	–	–	–	–	–	–
6	−2.8	16.4	−2.4	21.5	−1.8	30.1	−1.6	30.6
4	−1.7	15.7	−1.5	19.1	−1.1	23.4	−0.5	27.8
2	−0.5	15.5	−0.2	19.0	0.1	22.0	0.7	25.6
0	0.9	14.1	1.1	17.8	1.5	21.6	2.0	25.6
−4	3.4	14.7	3.6	19.2	–	–	–	–
−6	4.6	15.6	–	–	–	–	–	–
−8	6.1	16.9	–	–	–	–	–	–

Coordinates and angles of exit rays resulting from the computation are given in Table 1. They will be used later for the construction of the superposition image. Some of the ray trajectories as plotted by the computer are presented in Figures 4 and 5.

Axoparallel incident light (Fig. 4) is collected by the corneal lens. After entering the crystalline cone, the rays follow curved trajectories and come to a focus in the cone axis. The rays intersect each other between $x=31$ µm and $x=35$ µm with a smallest bundle diameter at $x=34$ µm. From there the rays diverge again and are gradually bent towards the axis so that they leave the cone again almost axoparallel. The maximal divergence of a ray from the axis is 1.1° in this bundle. The two outermost rays suffer total reflection at the cone boundary.

Incident parallel light bundles with input angles other than zero (4 examples are shown in Fig. 5) also form a focus each in the crystalline cone. The smallest bundle diameters are found between $x=34$ µm and $x=36$ µm. Their distance from the axis increases with the input angle. (The increase is in good approximation proportional to the tangent of the input angle.) The smallest bundle diameter does in no case exceed 0.6 µm. The rays leave the cone to the same side from which they entered the cornea. Thus, each ray follows an erect path. The exit angles (β) of rays in the same bundle differ somewhat. The maximal divergence of rays in one bundle is not more than 5° (except one ray in the bundle with $\alpha=18°$ where it is 8.5°).

The exit angle increases with the input angle (Fig. 6). The regression line has a slope of 1.32 (standard error 0.04, correlation coefficient 0.98). Thus, the investigated optical system can be said to have an angular magnification of 1.32 which is the same for all input angles.

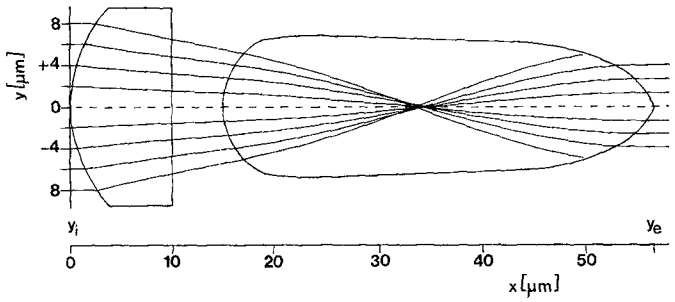

Fig. 4. Dioptric system consisting of cornea and crystalline cone with the coordinates and dimensions used in the model calculation. Starting $y(y_i)$ are defined for $x=0$ (cornea apex), exit $y(y_e)$ for $x=57{,}5\,\mu m$ (cone tip). Ray path for input angle $\alpha=0°$

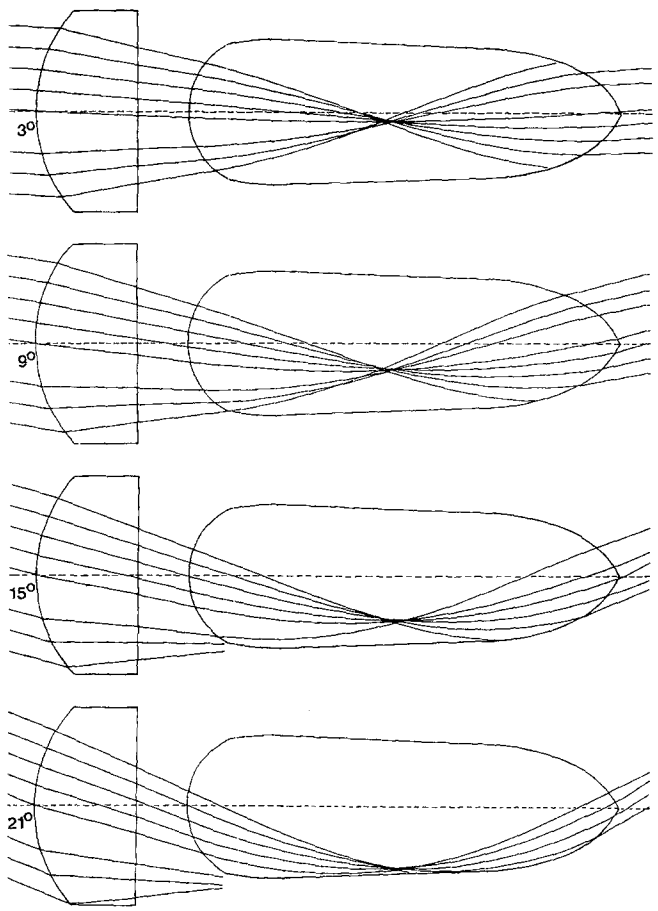

Fig. 5. Ray path for input angles α as indicated

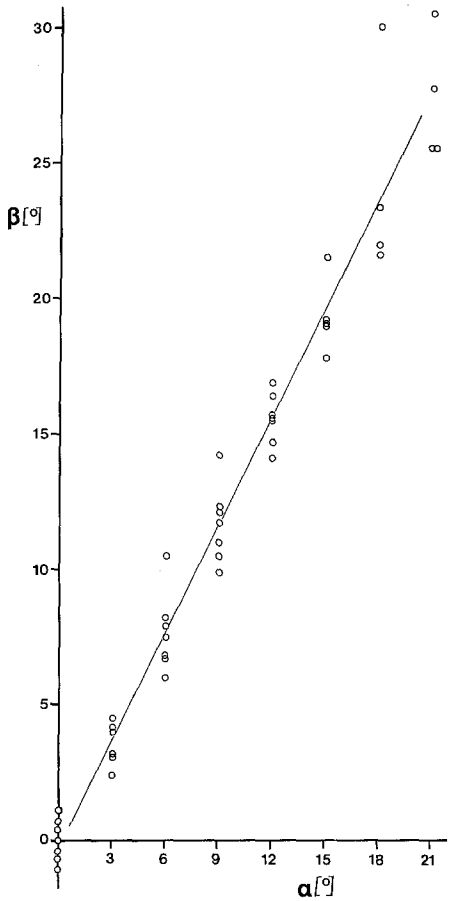

Fig. 6. Exit angle β versus input angle α with regression line

With input angles above 12° increasingly less rays are processed by the entire system due to the fact that rays begin to bypass the crystalline cone. This results in smaller diameters of exiting bundles. At an input angle of 22°, most of the eight investigated rays bypass the cone, two suffer total reflection, and only two rays leave the cone. No computed ray with an input angle of 23° or more passes through the entire cone. Thus, between 22° and 23° the limiting angle for ray processing of the system is reached.

Discussion

a) The Dioptric System

Vogt (1973) was able to show experimentally that the imaging quality of the cornea is limited by diffraction caused by the lens aperture and not by the dioptric properties of the corneal lens. I.e., lens errors can be neglected. A similar investigation of the crystalline cone is difficult and not available as yet. However, if we assume that for the entire system no bigger aperture than the cornea diameter is effective, diffraction limitation may be assumed for the

entire system. Consequently, the computation was performed only for rays incident in a meridional section and rays with oblique incidence were neglected. Nevertheless, a (laborious) three dimensional ray tracing and performance tests of the isolated dioptric system are desirable.

In our model, rays were neglected which suffered total reflection at the boundary cone surround. This total reflection was a necessary result of our model construction of the *Ephestia* dioptric system. In the material system, total reflection at this boundary must not necessarily occur and has not been observed up to now. The alternatives seem possible that either these rays are absorbed by pigment granules in the close vicinity of the cone or, with appropriate refractive indices surrounding the cone, continue outside the cone for some distance and then are absorbed by the pigment granules. Dense material in the cone sheeth and in the primary pigment cell (Fischer and Horstmann, 1971) is favouring this latter alternative. For lack of evidence, the rays in question were not processed further in our model. Even if totally reflected, they do not seem to be of determining influence on the performance of the system, although they certainly would deteriorate the superposition image. Deterioration could also be due to stray light of hitherto unknown origin in the eye. In addition, the image quality in our eye-cup preparations would be influenced by displacements of dioptric components during the experimental procedure. All these possible causes of image deterioration will show up when the propagated light is observed behind eye-cups. The photographed images in Figure 2 demonstrate that image deterioration in these preparations is limited. It may be presumed that this is even more so in the undisturbed eye.

The results of the ray path calculation is that the investigated optical system is in first approximation a telescopic system. It shows properties analogous to a Kepler telescope adjusted for infinity. Parallel entering light is focused in the plane of the intermediate image and leaves the system again parallel. The angular magnification is constant for all input angles. Different from a Kepler telescope, the ray path is not entirely produced by the refracting power of spherical lens surfaces. Here, a combination of refraction by curved surfaces (predominantly the cornea surface) with refraction by material of inhomogeneous refractive index (predominantly the crystalline cone) determines the path of the rays which, for the greater part of their way through the system, are not rectilinearly propagated. Direct optical observations on the *Ephestia* eye and optical apparatus are in full agreement with the existence of a Kepler telescope type system (Kunze, 1969, 1972b) with inhomogeneous imaging components (Kunze and Hausen, 1971; Vogt, 1973).

Previous ray tracings through the *Ephestia* dioptric system (Horridge, 1972) differ widely from the results presented here. However, those tracings were based on comparatively rough estimations of refractive indices and a discontinuous calculation of ray paths.

b) The Superposition Image

Superposition images have been repeatedly observed in insects (Coleoptera and Lepidoptera): Exner (1891) and Nunnemacher (1959, 1961) found them proximal

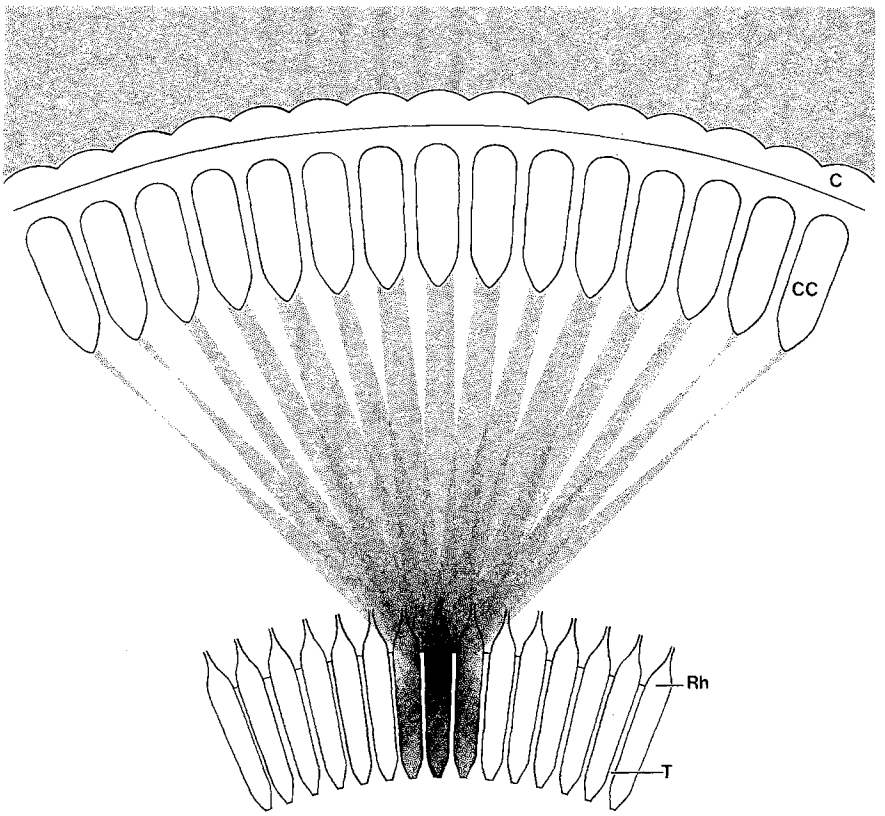

Fig. 7. Superposition of parallel incident light in the eye of *E. kühniella*. Exit light bundles as computed, histological structures adopted from Fischer and Horstmann (1971), eye radius from own measurements. *C*, cornea; *CC*, crystalline cone; *Rh*, rhabdom; *T*, tapetum

to the rhabdom layer, Kuiper (1962), Døving and Miller (1969), Horridge et al. (1972) in or close to it, whereas others (Eltringham, 1919; Winthrop and Worthington, 1966; Kunze, 1969) did not give definit positions.

Since different methods have been used in these investigations of which some may change the optical properties of the eye preparation, e.g., freeze sectioning or use of glycerin as mounting medium (see Vogt, 1973), wide differences in results are to be expected. In the present paper the fresh eye-cup was mounted on gelatine (Kuiper, 1962), which was shown by Hausen (1973) to preserve the optical properties of the crystalline cones.

For comparison with the position of the rhabdoms and the basal membrane in the *Ephestia* eye we refer to Fischer and Horstmann (1971). The total depth variation of superposition images as measured by us is 75 μm which is about 20 μm more than the rhabdom length. Almost all images were found distal to the position of the basal membrane. 80% of all superposition images were found to be within the region of the rhabdom, which extends from about 85 to 140 μm distance from the cone tip.

A second comparison can be drawn with our ray tracing in the dioptric

system of *Ephestia* which was based on the refractive index measurements of Hausen (1973) and Vogt (1974). From this model calculation, exit light bundles from different incident angles were selected so as to simulate parallel light falling onto the eye surface. In Figure 7 they are drawn leaving dioptric systems which are arranged at 3° intervals on a circle of 340 μm radius. (This eye radius we determined from tracings of the optically enlarged central eye curvature viewed from different directions.) The exit light bundles superimpose, the envelope forming a caustic curve.

There are two reasons for the caustic. One is a spherical aberration as stated by Exner (1891). If all dioptric systems are identical and arranged on a spherical surface, incident parallel light gives outgoing ray bundles which intersect the principal axis in different regions depending on the angle of the dioptric systems with the principal axis. The second reason is the non-parallelity of each bundle, increasing its diameter in the region of intersection above the exit diameter.

The smallest diameter formed by the intersecting bundles is the constructed superposition image of the incident parallel rays. For convenience we call it the "superposition focus". It is situated at a distance of 105 μm from the axial cone tip and is appr. 25 μm wide. On comparison with the eye anatomy the "superposition focus" is found to be the region of greatest rhabdom diameter. This is also the region where the distal extensions of the tapetum prevent further passage of light. The total extension of the "superposition focus" corresponds to about three rhabdom diameters.

Considering the differences of histological techniques, geometric optical measurements, and ray tracing on the basis of refraction index measurement the differences between the position of the superposition image, the "superposition focus", and the widest rhabdom diameter seem acceptable.

Thus, the superposition image is found at a distance from the cone tips which corresponds to the region of greatest rhabdom diameter; it may be presumed to be functional.

We thank Mrs. E. Ludwig for typing the manuscript, Mrs. I. Wolf and Ms. S. Nerlich for assistance in preparing the figures, and Prof. K. Kirschfeld for critically reading part of the manuscript.

References

Døving, K.B., Miller, W.H.: Function of insect compound eyes containing crystalline tracts. J. gen. Physiol. **54**, 250–267 (1969)

Eltringham, H.: Butterfly vision. Trans. Entom. Soc. Lond. **79**, 1–49 (1919)

Exner, S.: Die Physiologie der facettirten Augen von Krebsen und Insecten. Leipzig-Wien: Franz Deuticke 1891

Fischer, A., Horstmann, G.: Der Feinbau des Auges der Mehlmotte, *Ephestia kuehniella* Zeller (Lepidoptera, Pyralididae). Z. Zellforsch. **116**, 275–304 (1971)

Gerthsen, C.: Physik. Berlin-Heidelberg-New York: Springer 1966

Hausen, K.: Die Brechungsindices im Kristallkegel der Mehlmotte *Ephestia kühniella*. J. comp. Physiol. **82**, 365–378 (1973)

Horridge, G.A.: Further observations on the clear zone eye of *Ephestia*. Proc. roy. Soc. Lond. B **181**, 157–173 (1972)

Horridge, G.A., Giddings, L., Stange, G.: The superposition eye of skipper butterflies. Proc. roy. Soc. Lond. B **182**, 457–495 (1972)

Kuiper, J.W.: The optics of the compound eye. Symp. Soc. exp. Biol. **16**, 58–71 (1962)

Kunze, P.: Eye glow in the moth and superposition theory. Nature (Lond.) **223**, 1172–1174 (1969)
Kunze, P.: Comparative studies of arthropod superposition eyes. Z. vergl. Physiol. **76**, 347–357 (1972a)
Kunze, P.: Pigment migration and the pupil of the dioptric apparatus in superposition eyes. In: Information processing in the visual system of arthropods (ed. R. Wehner). Berlin-Heidelberg-New York: Springer 1972b
Kunze, P., Hausen, K.: Inhomogeneous refractive index in the crystalline cone of a moth eye. Nature (Lond.) **231**, 392–393 (1971)
Megitt, S., Meyer-Rochow, B.: Two calculations on optically non-homogeneous lenses. In: The compound eye and vision of insects (ed. G.A. Horridge). Oxford: Clarendon Press 1975
Nunnemacher, R.F.: The retinal image of arthropod eyes. Anat. Rec. **134**, 618–619 (1959)
Nunnemacher, R.F.: The structure and function of arthropod eyes. In: Progress in photobiology (eds. B. Ch. Christensen, B. Buchmann). Amsterdam: Elsevier Publishing Comp. 1961
Vogt, K.: Optische Untersuchungen an der Cornea der Mehlmotte *Ephestia kühniella*. J. comp. Physiol. **88**, 201–216 (1974)
Winthrop, J.T., Worthington, C.R.: Superposition image formation in insect eyes. Biophys. J. **6**, Proc. Bioph. Soc. p. 124 (1966)